LIMNOLOGY and OCEANOGRAPHY

ASLO

Limnol. Oceanogr. 66, 2021, 2393–2407

doi: 10.1002/lno.11760

Isotopic approaches to estimating the contribution of heterotrophic sources to Hawaiian corals

James T. Price,[1*] **Rowan H. McLachlan**,[1] **Christopher P. Jury**,[2] **Robert J. Toonen**,[2] **Andréa G. Grottoli**[1*]

[1]School of Earth Sciences, The Ohio State University, Columbus, Ohio
[2]Hawai'i Institute of Marine Biology, School of Ocean and Earth Science and Technology, University of Hawai'i at Mānoa, Honolulu, Hawai'i

Abstract

Corals obtain nutrition from the photosynthetic products of their algal endosymbionts and the ingestion of organic material and zooplankton from the water column. Here, we use stable carbon ($\delta^{13}C$) and nitrogen ($\delta^{15}N$) isotopes to assess the proportionate contribution of photoautotrophic and heterotrophic sources to seven Hawaiian coral species collected from six locations around the island of O'ahu, Hawai'i. We analyzed the $\delta^{13}C$ and $\delta^{15}N$ of coral tissues and their algal endosymbionts, as well as that of dissolved inorganic matter, particulate organic matter, and zooplankton from each site. Estimates of heterotrophic contribution varied among coral species and sites. Bayesian mixing models revealed that heterotrophic sources (particulate organic material and zooplankton) contributed the most to *Pocillopora acuta* and *Montipora patula* coral tissues at 49.3% and 48.0%, respectively, and the least to *Porites lobata* at 28.7%, on average. Estimates of heterotrophic contribution based on the difference between $\delta^{13}C$ of the host and algal endosymbiont ($\delta^{13}C_{h-e}$) and isotopic niche overlap often differed, while estimates based on $\delta^{15}N_{h-e}$ were slightly more aligned with the estimates produced using Bayesian mixing models. These findings suggest that the utility of each approach may vary with coral health status, regions, and coral species. Overall, we find that the mean heterotrophic contribution to Hawaiian coral tissues ranges from 20% to 50%, suggesting a variety of trophic strategies. However, these findings did not always match past direct measurements of heterotrophic feeding, indicating that heterotrophically acquired nutrition does not necessarily get incorporated into tissues but can be respired or exuded in mucus.

The function, growth, and overall health of most shallow-water reef-building corals are dependent on a fundamental relationship with their algal endosymbionts, Symbiodiniaceae (Muscatine and Porter 1977; LaJeunesse et al. 2018). The coral host benefits from the translocation of photoautotrophically derived organic carbon (C) and organic nitrogen (N) by their algal endosymbionts, while the algal endosymbionts benefit from heterotrophically derived C and N and respired C from the coral host to support growth and photosynthesis (e.g., Piniak et al. 2003; Hughes et al. 2010; Tanaka et al. 2015). Although the translocation of carbon from the algal endosymbionts can satisfy greater than 100% of coral daily metabolic demands (e.g., Muscatine et al. 1984; Edmunds and Davies 1989; Grottoli et al. 2006), healthy corals can also fulfill between 5% and 50% of their daily metabolic demands through the capture and assimilation of organic matter and plankton from the water column (e.g., Palardy et al. 2008; Houlbrèque and Ferrier-Pagès 2009; Grottoli et al. 2014). Indeed, heterotrophy is a vital component of coral trophic strategies, as the heterotrophic capacity of a coral is a key contributor to their resistance to bleaching and resilience following bleaching events (e.g., Grottoli et al. 2006; Anthony et al. 2009; Conti-Jerpe et al. 2020). However, determining the proportionate contribution of photoautotrophic and heterotrophic sources to coral diets is complicated as heterotrophic effort and the nutritional sources available to corals in the marine environment can vary with upwelling (Palardy et al. 2005; Radice et al. 2019), turbidity (e.g., Anthony 1999; Anthony and Fabricius 2000), primary productivity (Fox et al. 2018), lunar cycle (Palardy et al. 2006), coral surface area to volume ratio (Palardy et al. 2005), and water flow rates (Ribes and Atkinson 2007; Wijgerde et al. 2012). The recycling of C, N, and phosphorous between the coral host and its algal endosymbiont (e.g., Hughes

*Correspondence: price.1118@osu.edu (J.T.P.); grottoli.1@osu.edu (A.G.G.)

Additional Supporting Information may be found in the online version of this article.

et al. 2010; Hughes and Grottoli 2013; Tanaka et al. 2018) further complicates interpretations of trophic strategies among corals.

Direct measurements of photosynthesis, respiration, and feeding rates are often used to assess the contributions of photoautotrophy and heterotrophy to the daily metabolic demands of corals (e.g., Anthony and Fabricius 2000; Grottoli et al. 2006; Grottoli et al. 2014). However, these methods can be costly, labor-intensive, and destructive. Further, direct measurements of photosynthesis and feeding rate may not translate to the ultimate incorporation of those nutritional resources into coral tissue. For example, the allocation of autotrophic or heterotrophic sources to host and algal endosymbiont tissues can vary with prior thermal and nutritional regimes (e.g., Hughes et al. 2010; Baumann et al. 2014; Krueger et al. 2018).

Alternatively, natural abundance stable carbon ($\delta^{13}C$) and nitrogen ($\delta^{15}N$) isotopes of the coral host and algal endosymbionts can be used to broadly estimate the proportionate contribution of photoautotrophy and heterotrophy to coral tissues under natural and experimental conditions (e.g., Muscatine et al. 1989; Rodrigues and Grottoli 2006; Ferrier-Pagès et al. 2011). Trophic strategies of corals have also been identified using tissue stable isotopes in corals from Hong Kong (Conti-Jerpe et al. 2020), the South China Sea (Xu et al. 2020), and Maldives (Radice et al. 2019), and shown to vary along a natural gradient of primary productivity among the Southern Line Islands in the Central Pacific (Fox et al. 2018). However, unlike some other ecological disciplines, isotope mixing model approaches have not been widely adapted in coral research to evaluate the proportionate contribution of nutritional sources to coral diets.

Heterotrophic plasticity and/or high baseline heterotrophic capacity have been associated with lower susceptibility to, and faster recovery from, heat stress (e.g., Grottoli et al. 2006; Hughes and Grottoli 2013; Conti-Jerpe et al. 2020). Knowing baseline heterotrophic contributions to coral tissues could be important when determining which species are more likely to survive climate change and are better candidates for coral restoration and conservation efforts. Here, we use four approaches with stable carbon and nitrogen isotopes to determine the proportionate contribution of various nutritional sources to the tissues of seven species of Hawaiian corals as follows: (1) we calculated the difference between the carbon isotope values of both the coral host and algal endosymbiont (sensu Muscatine et al. 1989), (2) we calculated the difference between the nitrogen isotope values of both the coral host and algal endosymbiont (sensu Nahon et al. 2013), (3) estimated the contribution of heterotrophy to coral tissues by calculating the overlap between the isotopic composition of the coral host and algal endosymbiont (sensu Conti-Jerpe et al. 2020), and (4) estimated the proportionate contribution of different nutritional resources to corals surrounding the island of Oʻahu using a Bayesian mixing model. To assess the possible effect of variable environmental conditions on the contribution of photoautotrophic and heterotrophic sources to these corals, we also compared the mean estimated contribution of each source to each coral species from collection sites around Oʻahu.

Materials and methods

Coral sampling

Corals were collected between 17 August and 13 November 2015 from six sites (Electric Beach, Haleʻiwa, Hawaiʻi Institute of Marine Biology [HIMB], Magic Island, Sampan, and Waimānalo) surrounding the island of Oʻahu, Hawaiʻi (HI), U.S.A. (Supporting Information Fig. S1). Typical environmental conditions at each collection site are summarized in Table S1. Methods used to collect the environmental data are summarized in the Supporting Information. Ramets of seven coral species (*Montipora capitata*, *Montipora patula*, *Pocillopora acuta*, *Pocillopora meandrina*, *Porites compressa*, *Porites evermanni*, and *Porites lobata*) were collected at a depth of 0.5–5 m (Table S2). The vast majority of corals were collected at a depth of 2 ± 1 m, but small differences in reef geomorphology among sites required a few colonies to be collected from slightly shallower (0.5–1 m; HIMB and Sampan) or deeper (3–5 m; Electric Beach and Haleʻiwa). A 5–10 cm coral ramet (branch or mound) was removed underwater via hammer and chisel from parent colonies separated by at least 5 m on the reef to minimize the possibility of selecting corals of the same genet (Baums et al. 2019). Corals were only sampled from sites where they were relatively abundant, and therefore not all coral species were sampled at every site (*see* Table S2 for the number of samples collected per site and species). Upon sampling in the field, each coral ramet was bagged in seawater collected adjacent to the colony for subsequent live transport to HIMB. Following transport (~ 2 h), each ramet was immediately frozen at −20°C, and later shipped to The Ohio State University on dry ice where they were stored at −80°C. Methods for separating coral host and algal endosymbiont tissues for isotopic analyses are described in Price et al. (2020) and in the Supporting Information.

Source sampling

Sampling of potential sources of carbon and nitrogen to corals was not performed at the time of the coral collection due to logistical constraints. Between 06 December 2017 and 16 December 2017, water and zooplankton (150–800 μm) samples were collected at 0.5–1.0 m depth, close to corals from each site. Up to 8 L of seawater was collected at least once from each site (twice from HIMB) in preacidified 2-liter brown Nalgene bottles during the day (12:00–14:00 h) and night (18:00–20:00 h) and placed on ice in a cooler. Seawater was subsampled from the Nalgene bottles within 4 h of collection, filtered through prebaked quartz microfiber filters, and preserved for stable isotope analysis of dissolved inorganic matter (DIM) and particulate organic matter (POM). Specifically, dissolved inorganic carbon (DIC), particulate organic carbon, and particulate organic nitrogen (PON) were analyzed

according to established methods (e.g., Moyer et al. 2013) and are described further in the Supporting Information. Low N amounts in POM samples from Sampan and Electric Beach resulted in measurements of $\delta^{15}N$ of POM from only the other four sites. Zooplankton samples were only collected during the nighttime sampling at four of the six sites, as surf conditions at Haleʻiwa and Electric Beach were unsafe during the sampling period. To collect zooplankton, a bucket with an illuminated dive torch affixed to the bottom was placed on the seafloor near the reef at 1 m depth for 5 min. The zooplankton were separated into 400–800 μm and 150–400 μm size fractions in the field, stored on ice, and then isolated onto a glass fiber filter and stored at −20°C upon return to the lab the same day. Details of the isotopic analysis of the source samples are described in the Supporting Information.

Statistical analyses

All analyses were performed using R software package version 4.0.3 (R Core Team 2020). Statistical significance was defined as $\alpha \leq 0.05$. All isotopic data are available at the Biological and Chemical Oceanography Data Management Office repository (Grottoli 2020, 2021).

Approach 1 and 2: Stable carbon and nitrogen isotopes of the host minus endosymbiont

The difference between the $\delta^{13}C$ of the host tissue ($\delta^{13}C_h$) and the algal endosymbionts ($\delta^{13}C_e$) (henceforth referred to as $\delta^{13}C_{h-e}$) values were computed (e.g., Muscatine et al. 1989; Rodrigues and Grottoli 2006; Grottoli et al. 2017). Higher $\delta^{13}C_{h-e}$ values typically indicate that photosynthesis contributes a larger proportion of fixed carbon to coral tissues than heterotrophy, and vice versa. Recent evidence suggests that $\delta^{15}N_h$–$\delta^{15}N_e$ (henceforth referred to as $\delta^{15}N_{h-e}$) is also informative of the source contributions to coral tissues (e.g., Nahon et al. 2013; Conti-Jerpe et al. 2020). Here, $\delta^{13}C_{h-e}$ and $\delta^{15}N_{h-e}$ were each compared among coral species using a nonparametric Kruskal-Wallis test followed by a post hoc Dunn's test, as normality and homoscedasticity of variance could not be achieved.

Approach 3: Stable isotope Bayesian ellipses

Using the R package SIBER (Stable Isotope Bayesian Ellipses in R v2.1.5) (Jackson et al. 2011), maximum likelihood ellipses encompassing 40% of the variation were fitted to the overall isotopic values of the host and algal endosymbiont tissue. To determine the trophic strategy, the area and amount of overlap were calculated between host and algal endosymbiont standard ellipse areas corrected for sample size (SEA_C), as a proportion of the host SEA_C (Conti-Jerpe et al. 2020; Santos et al. 2021). The overlap was also calculated for ellipses encompassing 95% of the host and algal endosymbiont data to account for a greater amount of variation within each species. Hoteling t^2 tests with 999 permutations were used to determine whether the centroid (multivariate mean) isotopic composition of the overall dataset of host and algal endosymbiont differed within each coral species via the R package, *Hotelling* v1.0-5.

Approach 4: Bayesian mixing models

The proportionate contribution of DIM, POM, and zooplankton to whole coral tissues was estimated using the Bayesian isotope mixing models via the R package, MixSIAR v3.1.12 (Stock et al. 2018). Since C and N recycling is rapid and continuous between the host and algal endosymbiont in corals (e.g., Tremblay et al. 2012; Tanaka et al. 2015; Rangel et al. 2019), the mixing models were performed using whole coral samples (host and algal endosymbiont together) as the consumer. Because potential C and N sources were only sampled once around Oʻahu or were derived from the literature (Table 1), DIM, POM, and zooplankton isotopic values were averaged across sites. The $\delta^{15}N$ of dissolved inorganic nitrogen (DIN) was estimated via $\delta^{15}N$ of nitrate in Kāneʻohe Bay, as these were the only published values found for the island of Oʻahu (Wall et al. 2019). While ammonium can also be a source of inorganic nitrogen to corals, $\delta^{15}N$ of ammonium can be highly variable and $\delta^{15}N$ of nearby ammonium had not been measured. In addition, dissolved organic matter (DOM) was not included in the mixing models because (1) the isotopic values were similar to those measured in POM, making it difficult for the models to differentiate dietary contribution between the two sources, and (2) we did not measure the $\delta^{15}N$ of DOM and we were unable to locate reliable

Table 1. Summary of mean $\delta^{13}C$ and $\delta^{15}N$ values (mean ± SD) and fractionation or trophic discrimination factors (TDF) for each of the sources surrounding Oʻahu, HI.

	DIM		POM		Zooplankton (150–800 μm)	
	$\delta^{13}C$ (‰)	$\delta^{15}N$ (‰)	$\delta^{13}C$ (‰)	$\delta^{15}N$ (‰)	$\delta^{13}C$ (‰)	$\delta^{15}N$ (‰)
Measured or estimated value	0.52 ± 0.14*	4.30 ± 1.00†	−21.24 ± 0.83*	2.87 ± 1.58*	−18.42 ± 1.68*	6.45 ± 0.68*
TDF	−12.10 ± 3.00‡	0.00 ± 0.00§	1.00 ± 1.00	3.40 ± 1.00‖	1.00 ± 1.00	3.40 ± 1.00‖

*This study.
†$\delta^{15}N$ of DIN for Oʻahu from nitrate collected in Kāneʻohe Bay by Wall et al. (2019).
‡Estimated fractionation value of $\delta^{13}C$-DIC incorporated into whole coral and endosymbiont tissue from Swart et al. (2005).
§Absence of a $\delta^{15}N$ TDF for DIN incorporation into whole coral and algal endosymbionts from Muscatine and Kaplan (1994).
‖Estimated fractionation value of $\delta^{15}N$ between trophic levels from Minagawa and Wada (1984) and Post (2002).

nearshore datasets with $\delta^{15}N$ of DOM surrounding the Hawaiian islands. We speculate that DOM accounts for a portion of the estimated contribution from POM in these mixing models. Additional details about the mixing model procedures, source values, and information about fractionation and trophic discrimination factors (TDFs) are described in the Supporting Information. Pearson's correlations were used to test for relationships between the mean estimated proportionate contribution of heterotrophy (POM + zooplankton) with $\delta^{13}C_{h-e}$, $\delta^{15}N_{h-e}$, and the percent overlap of 40% SEA_C values among all coral species, with the mean values for each species used to build the correlations.

Results

The mean isotopic composition (i.e., $\delta^{13}C$ and $\delta^{15}N$) of whole coral, host tissue, and algal endosymbiont values for each species and site are presented in Supporting Information Tables S3, S4. The average $\delta^{13}C$ and $\delta^{15}N$ values of DIM, POM, and zooplankton are shown in Table 1. These data were used to evaluate the four approaches listed below.

Approach 1: Stable carbon isotopes of the host minus endosymbiont

The mean $\delta^{13}C_{h-e}$ ranged from -0.34 ± 0.63‰ to 2.23 ± 0.81‰ among all species and sites (Fig. 1A–G; Supporting Information Table S3). The $\delta^{13}C_{h-e}$ differed significantly among coral species of different genera, but not always among species within the same genus (Supporting Information Table S5A). Of the seven species, *M. capitata* and *M. patula* had the greatest mean $\delta^{13}C_{h-e}$ values of 1.53 ± 0.63‰ and 1.35 ± 0.69‰, respectively, while *P. meandrina* and all three *Porites* species had the lowest mean values near 0‰.

Approach 2: Stable nitrogen isotopes of the host minus endosymbiont

The mean $\delta^{15}N_{h-e}$ ranged from -1.92 ± 0.55‰ to 2.29 ± 0.55‰ across all species and sites (Fig. 1H–N; Supporting Information Table S4). The $\delta^{15}N_{h-e}$ differed among species, but these differences were not always delineated by genera (Supporting Information Table S5B). *M. patula* and *P. acuta* corals had the greatest mean $\delta^{15}N_{h-e}$ values at 1.23 ± 0.66‰ and 1.42 ± 0.95‰, respectively, while *P. evermanni* had the lowest mean value of -1.79 ± 0.68‰.

Approach 3: Stable isotope Bayesian ellipses

Overlap between 40% SEA_C of the host and algal endosymbionts ranged from 0.0% to 60.5% as a proportion of host SEA_C across all species (Fig. 2; Supporting Information Table S6). Lower 40% SEA_C overlap values indicated relatively low amounts of resource sharing between the coral and algal endosymbiont partners and a higher estimated contribution of heterotrophic resources to coral tissues. Overlap patterns for the 40% SEA_C were not always conserved within a coral genus, as the two species with the greatest overlap were *P. meandrina* (60.5%) and *P. lobata* (52.0%), while *M. patula* and *P. evermanni* had 1.1% and 0.0% overlap between host and algal endosymbiont tissues, respectively. Interestingly, these latter two species displayed opposite patterns in their measured isotopic values, as the mean $\delta^{15}N$ of the host was enriched over the algal endosymbiont in *M. patula*, but the host $\delta^{15}N$ was depleted relative to the symbiont in *P. evemanni* (Fig. 2B,G). In addition, the overall isotopic composition of the host and algal endosymbiont tissues differed significantly within all coral species except for except *P. meandrina* whose 40% SEA_C values overlapped the most (Supporting Information Table S7). The 95% SEA_C was also considered to account for variation across the whole data set. While *M. patula* and *P. evermanni* remained the corals with the lowest amount of overlap, the range of SEA_C values was much more constrained from 40.1% to 71.3%.

Approach 4: Bayesian mixing models

The proportionate contribution of each source to whole coral tissue was estimated with MixSIAR. When considering all corals together, heterotrophy (POM + zooplankton) contributed a mean of 34.0%, while DIM contributed an estimated mean of 66.0% to whole coral tissue (Supporting Information Table S8A; Fig. 3). However, when each species was considered separately, heterotrophy had the highest estimated mean contribution to *P. acuta* of 49.3% and the lowest mean contribution to *P. lobata* of 28.7% (Figs. 4, 5; Supporting Information Table S8D,G). POM was estimated to be the most consistently incorporated heterotrophic source in corals at 18.3–46.9%, rather than zooplankton (0.7–10.4%) (Supporting Information Table S8B–H). To account for the possibility that there was minimal trophic enrichment of $\delta^{13}C$ and $\delta^{15}N$ in the available heterotrophic sources due to the recycling of C and N between the host and algal endosymbiont, mixing models were also produced using TDF values of zero for POM and zooplankton. With TDF values of zero, mean estimated contribution of heterotrophy increased by only $2.5\% \pm 4.2\%$, but mean estimated contribution of zooplankton increased from $3.0\% \pm 3.4\%$ to $21.3\% \pm 12.4\%$ across all species (Supporting Information Table S9B–H).

Within each species, site-specific differences in the estimated proportionate contribution of each source were observed (Fig. 4). The mean estimated proportionate contribution of heterotrophy to *M. capitata* from Hale'iwa was 9.6% vs. 35.4% at the other collection sites, resulting in a higher proportionate contribution of DIM to those corals at Hale'iwa than their conspecifics around O'ahu (Fig. 4A). Although the differences were often small, Magic Island corals had the lowest estimated mean contribution of heterotrophy to their tissues in four of the five species collected there (*P. meandrina*, *P. compressa*, *P. lobata*, and *P. evermanni*, but not *P. acuta*, *see* Supporting Information Table S8). The mean estimated proportionate contribution of heterotrophy to *P. evermanni* from Sampan was 52.7% vs. an average of 26.9% at the other collection sites, resulting in a lower proportionate contribution of DIM to those corals at Sampan than their conspecifics around O'ahu. Corals from HIMB (*M. capitata*, *P. acuta*, *P. compressa*) had consistently high proportionate contributions of

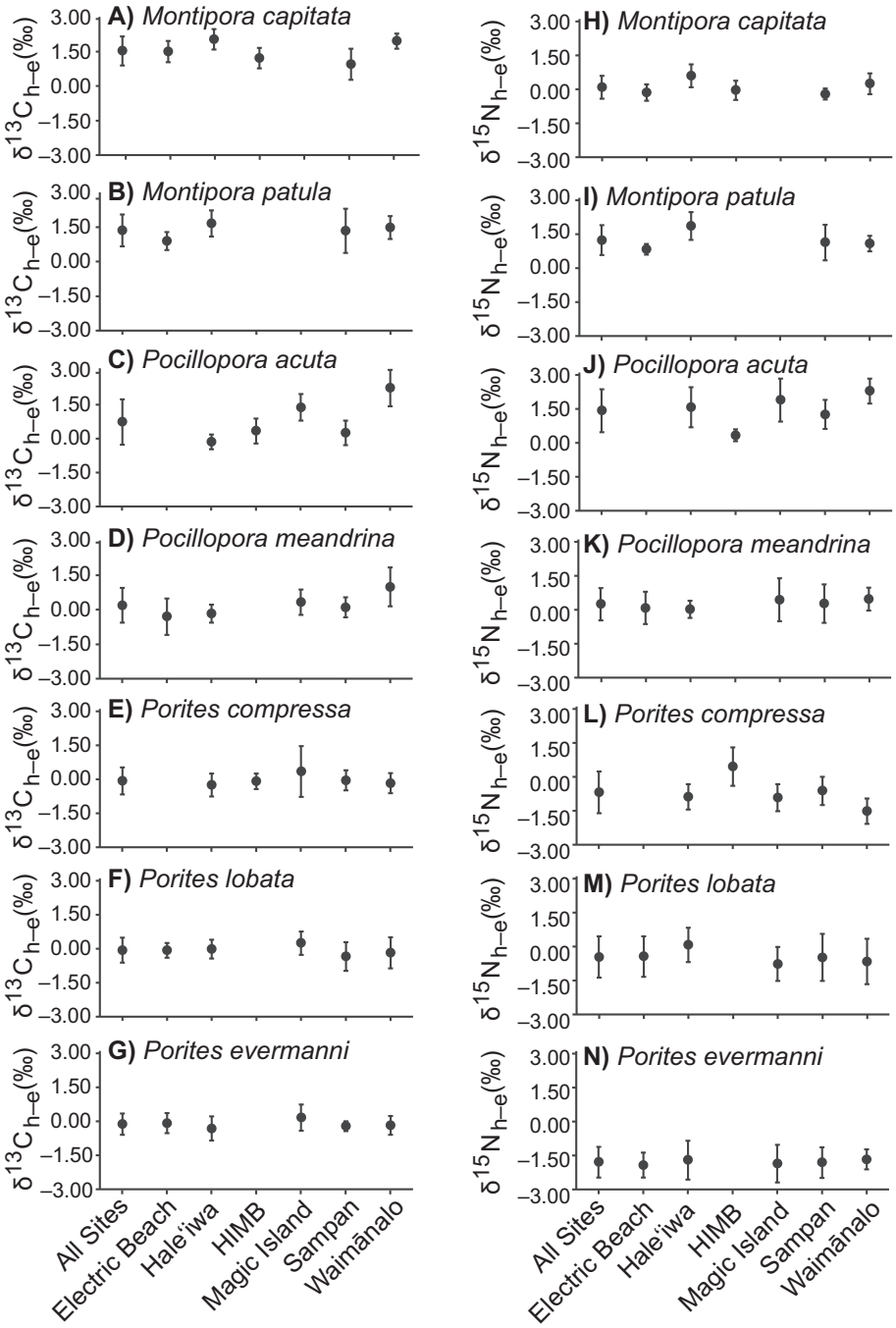

Fig. 1. Mean (± SD) $\delta^{13}C$ of the coral host—$\delta^{13}C$ of the endosymbiont ($\delta^{13}C_{h-e}$, approach 1) in (**A**) *Montipora capitata*, (**B**) *Montipora patula*, (**C**) *Pocillopora acuta*, (**D**) *Pocillopora meandrina*, (**E**) *Porites compressa*, (**F**) *Porites lobata*, and (**G**) *Porites evermanni* and $\delta^{15}N$ of the coral host—$\delta^{15}N$ of the endosymbiont ($\delta^{15}N_{h-e}$, approach 2) in (**H**) *Montipora capitata*, (**I**) *Montipora patula*, (**J**) *Pocillopora acuta*, (**K**) *Pocillopora meandrina*, (**L**) *Porites compressa*, (**M**) *Porites lobata*, and (**N**) *Porites evermanni* from all collection sites surrounding O'ahu, HI.

heterotrophy to their tissues relative to these corals at most other sites (Supporting Information Table S8). Overall, most differences in photoautotrophic vs. heterotrophic contribution to coral tissues were species-specific and patterns among provenance were often inconsistent.

Discussion

Here, we assessed the proportionate contribution of organic sources (derived through heterotrophy by the coral animal host) and inorganic sources (derived primarily through photosynthesis and inorganic uptake by the algal endosymbionts) to the

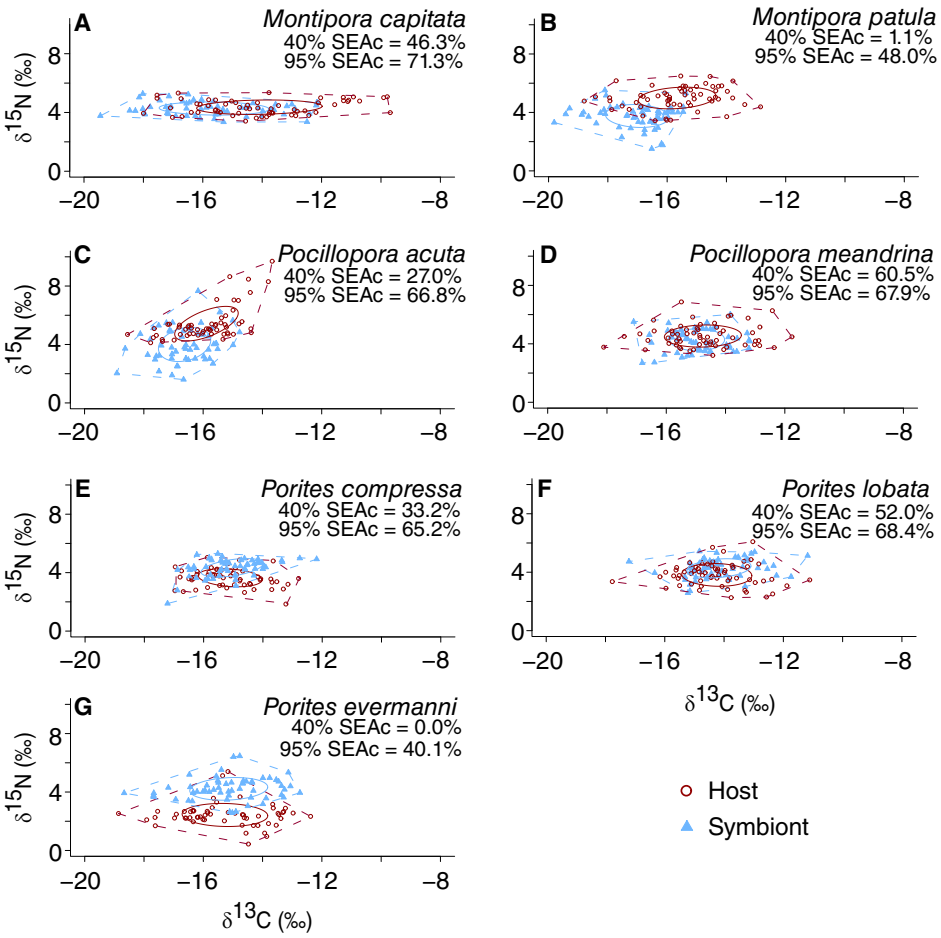

Fig. 2. Results of SIBER (approach 3) analysis showing biplots of $\delta^{13}C$ and $\delta^{15}N$ for (**A**) *Montipora capitata*, (**B**) *Montipora patula*, (**C**) *Pocillopora acuta*, (**D**) *Pocillopora meandrina*, (**E**) *Porites compressa*, (**F**) *Porites lobata, and* (**G**) *Porites evermanni* collected surrounding Oʻahu, HI. The solid ellipses encompass 40% of variability in the host and algal endosymbiont groups, while dotted lines encompass 100% of the variability in each group. Degree of overlap calculated from standard ellipse area corrected for sample size (SEA_C), both 40% and 95%, as a proportion of host SEA_C suggests the potential for resource sharing between the coral host and algal endosymbiont. Generally, greater overlap represents relatively high sharing of dietary resources incorporated into tissues between the host and its algal endosymbionts, while lower overlap represents relatively low sharing of dietary resources between the symbiotic partners.

tissue of seven Hawaiian coral species from six sites surrounding Oʻahu, Hawaiʻi. We compared four isotopic approaches (Fig. 6) and found that overall, coral tissues are 3.0–57.4% derived from heterotrophic sources depending on the coral species, location, and statistical approach used as discussed below.

Approach 1: Stable carbon isotopes of the host minus endosymbiont

The utility of this approach for estimating the proportionate contribution of heterotrophic and photoautotrophic carbon to coral tissues is well established. The $\delta^{13}C_{h-e}$ values of coral often decrease with depth (e.g., Muscatine et al. 1989; Alamaru et al. 2009; Williams et al. 2018) or following bleaching (e.g., Rodrigues and Grottoli 2006; Schoepf et al. 2015; Wall et al. 2019), and can also decrease with seawater productivity (Fox et al. 2018). Decreases in $\delta^{13}C_{h-e}$ have often been interpreted as a function of increases in the proportionate contribution in heterotrophic carbon to coral tissues (e.g., Muscatine et al. 1989; Rodrigues and Grottoli 2006; Schoepf et al. 2015), but can also relate to other factors, such as the ratio of protein : lipid : carbohydrate in coral tissues (Wall et al. 2019). Among the seven species, average $\delta^{13}C_{h-e}$ values were highest in the two *Montipora* species, intermediate in the two *Pocillopora* species, and lowest in the *Porites* corals (Figs. 1A, 6A). Low $\delta^{13}C_{h-e}$ values indicate the highest proportionate contribution of heterotrophically derived carbon to coral tissues (Fig. 6A). In the montiporids, the $\delta^{13}C_{h-e}$ values were 1–2‰ higher than previously reported for nonbleached Hawaiian *M. capitata* (Rodrigues and Grottoli 2006; Wall et al. 2020), but consistent with past studies showing that baseline feeding rates are low and the contribution of heterotrophic carbon relative to daily respiratory demand (CHAR, Grottoli

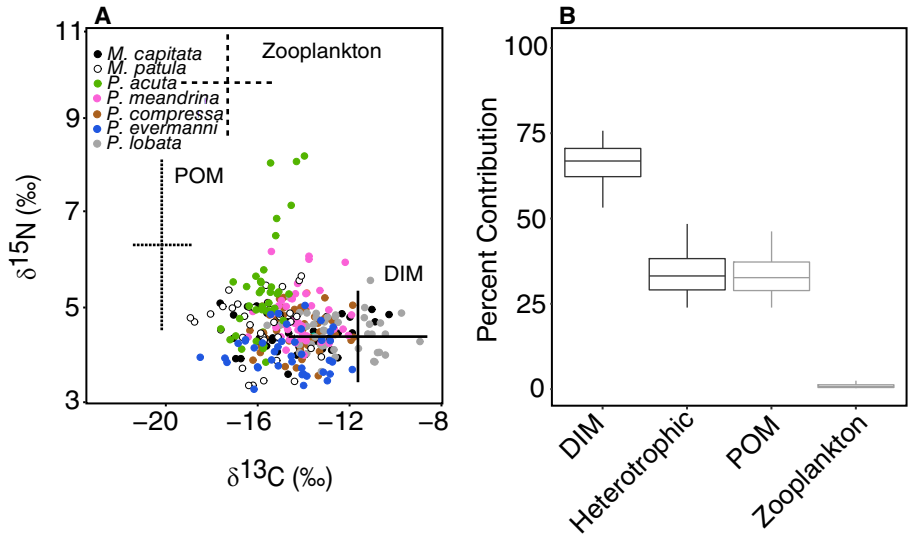

Fig. 3. (**A**) Isotope biplot for the seven sampled species in Oʻahu, HI. Each source is plotted with fractionation and trophic discrimination factors considered (*see* Table 1). (**B**) Posterior probabilities of the proportionate contribution of each source as determined by MixSIAR for all species combined (approach 4), and where the total heterotrophic contribution is the sum of the POM and zooplankton contributions. The horizontal line at the center of each box is the median, with boxes extending to 25% and 75% credible intervals and whiskers representing the 5% and 95% credible intervals. The corresponding MixSIAR output is listed in Supporting Information Table S8A.

et al. 2006) is only 18% in nonbleached *M. capitata* (Grottoli et al. 2006; Palardy et al. 2008).

In the *Porites* species, the low $\delta^{13}C_{h-e}$ values were similar to those previously reported for nonbleached *P. lobata*, *P. compressa*, and *Porites astreoides* (Rodrigues and Grottoli 2006; Levas et al. 2013; Levas et al. 2018), and consistent with past studies showing that baseline feeding rates were moderate and zooplankton CHAR values were 30–70% in *P. compressa*, *P. lobata*, and *P. astreoides* corals (Palardy et al. 2008; Grottoli et al. 2014; Levas et al. 2016). However, $\delta^{13}C_{h-e}$ alone may be more indicative of the proportion of resources shared rather than a measure of heterotrophic contribution to tissues. For example, *P. evermanni* from Sampan were depleted by 2‰ in both $\delta^{13}C_h$ and $\delta^{13}C_e$ relative to conspecifics from Waimānalo, but the $\delta^{13}C_{h-e}$ values at both sites were near 0‰, possibly obscuring a difference in heterotrophic contribution between these sites (Supporting Information Table S3).

There are other factors that could account for some of the variability in $\delta^{13}C_{h-e}$ that are unrelated to heterotrophy. For instance, the type of algal endosymbiont often differs among and within coral species (e.g., LaJeunesse et al. 2004), which may affect the isotopic fractionation and resulting isotopic composition of the coral (Wall et al. 2020). Algal endosymbiont density can also correlate with $\delta^{13}C_e$ values, as seen in Hawaiian *M. capitata* (Wall et al. 2020). One way to partially reduce the influence of these factors would be to only compare $\delta^{13}C_{h-e}$ within species. Further, methods like compound-specific isotope analysis of essential amino acids could provide a robust tool for more precisely identifying contributions from multiple sources (e.g., Fox et al. 2019; Fujii et al. 2020; Ferrier-Pagès et al. 2021).

Approach 2: Stable nitrogen isotopes of the host minus endosymbiont

The patterns found using $\delta^{15}N_{h-e}$ did not closely match those observed using $\delta^{13}C_{h-e}$ (Figs. 1H–N, 6B), particularly when interpreting these approaches as they have been used in past studies. However, interpreting the proportionate contribution of heterotrophy and photoautotrophy using $\delta^{15}N_{h-e}$ is less established than for $\delta^{13}C_{h-e}$ (Nahon et al. 2013). Based on $\delta^{15}N_{h-e}$, the montiporid corals appeared more heterotrophic and the poritid corals less heterotrophic than indicated by the $\delta^{13}C_{h-e}$ results (Fig. 6A,B), and species of the same genus were often separated by more than 1‰ (e.g., $\delta^{15}N_{h-e}$ was lower in *M. capitata* than *M. patula*). Yet, the $\delta^{15}N_{h-e}$ of ~ 0‰ for *M. capitata* was similar to the calculated value based on previously reported $\delta^{15}N_h$ and $\delta^{15}N_e$ values for that species (Rodrigues and Grottoli 2006), which is consistent with low baseline heterotrophy in nonbleached *M. capitata* (Grottoli et al. 2006; Palardy et al. 2008). In the *Porites* corals, the slightly negative $\delta^{15}N_{h-e}$ values of *P. compressa* are approximately 0.5–1.0‰ lower than the calculated values based on previously reported $\delta^{15}N_h$ and $\delta^{15}N_e$ values in Hawaiʻi (Rodrigues and Grottoli 2006), but the $\delta^{15}N_{h-e}$ of *P. lobata* matches previously reported values in Hawaiʻi (Levas et al. 2013). This suggests that $\delta^{15}N_{h-e}$ is generally negative or near zero in *Porites* corals and may not be reflective of their previously reported moderate feeding rates and CHAR (e.g., Rodrigues and Grottoli 2006; Palardy et al. 2008). This implies that much of the heterotrophic matter may not be incorporated into tissues but is instead respired to meet metabolic demand or exuded as mucus (e.g., Hughes et al. 2010; Levas et al. 2016; Tanaka et al. 2018). Indeed, some studies have

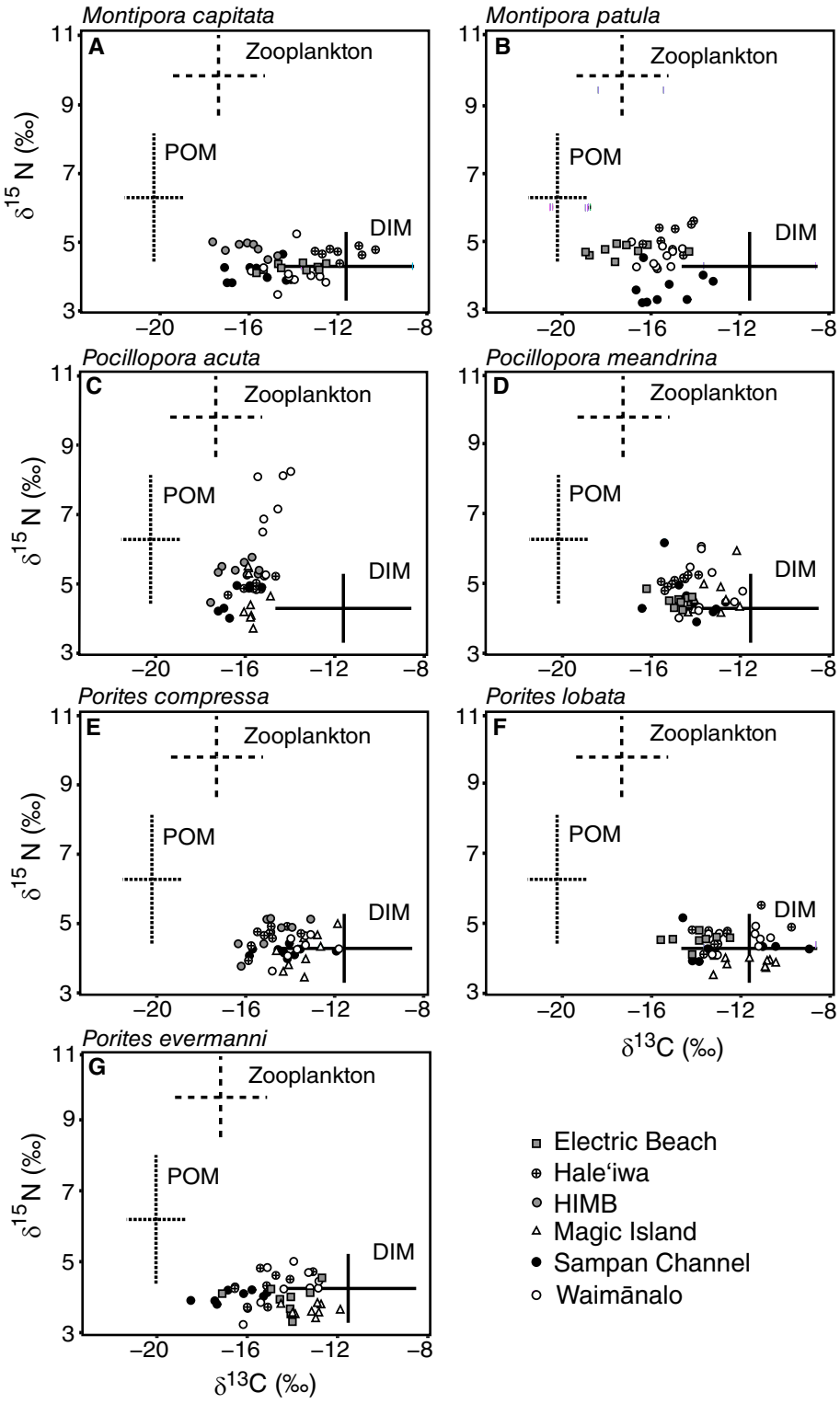

Fig. 4. Isotope biplot for (**A**) *Montipora capitata*, (**B**) *Montipora patula*, (**C**) *Pocillopora acuta*, (**D**) *Pocillopora meandrina*, (**E**) *Porites compressa*, (**F**) *Porites lobata*, and (**G**) *Porites evermanni* from each site in O'ahu, HI (approach 4). Each source is plotted with fractionation and trophic discrimination factors considered (*see* Table 1).

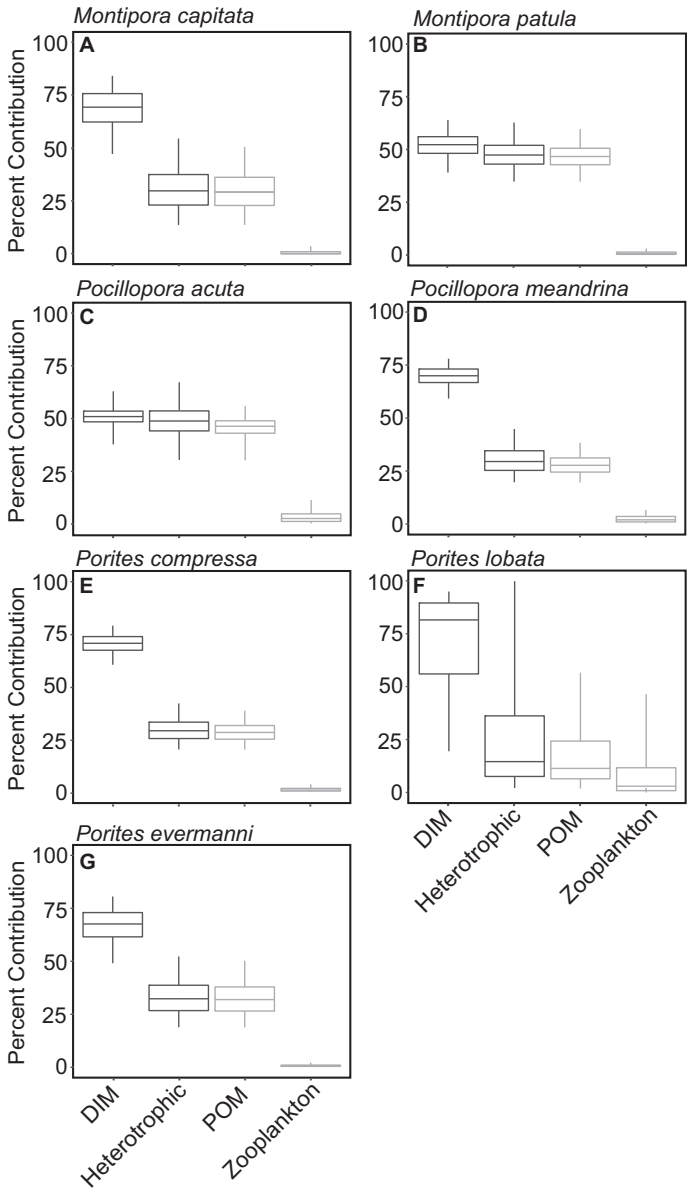

Fig. 5. Posterior probabilities of the proportionate contribution of each source (heterotrophic = POM + zooplankton) as determined by MixSIAR (approach 4) for (**A**) *Montipora capitata*, (**B**) *Montipora patula*, (**C**) *Pocillopora acuta*, (**D**) *Pocillopora meandrina*, (**E**) *Porites compressa*, (**F**) *Porites lobata*, and (**G**) *Porites evermanni* in Oʻahu, HI. The horizontal line at the center of each box is the median, with boxes extending to 25% and 75% credible intervals and whiskers representing the 5% and 95% credible intervals. The corresponding MixSIAR output is listed in Supporting Information Table S8B–H.

found that the $\delta^{15}N_{h-e}$ values likely show the opposite relationship to $\delta^{13}C_{h-e}$, such that $\delta^{15}N_{h-e}$ increases with greater proportionate contribution of heterotrophy, due to trophic enrichment of the host tissues ($\sim$ 3.4‰ $\delta^{15}N$) expected with the assimilation of dissolved organic nitrogen, PON, and zooplankton (Ferrier-Pagès et al. 2011; Conti-Jerpe et al. 2020). However, in a laboratory study, increased feeding resulted in a decrease in approximately 0.5‰ $\delta^{15}N$ in the host tissue, suggesting no trophic enrichment (Reynaud et al. 2009). The relatively slow N turnover time of 3–12 months in coral tissues (Tanaka et al. 2018; Rangel et al. 2019) may also be contributing to variability in the interpretations of $\delta^{15}N_{h-e}$. Because the endosymbiont cells are typically expelled during bleaching, a significant shift in $\delta^{15}N_{h-e}$ may occur immediately following bleaching, whereas shifts in $\delta^{15}N_{h-e}$ of nonbleached corals may be less pronounced and/or require longer periods of time to fully turnover (Reynaud et al. 2009; Ferrier-Pagès et al. 2011; Radice et al. 2019). Thus, coral health status should be considered when interpreting $\delta^{15}N_{h-e}$ values.

The isotopic composition of these corals could also relate to coral morphology or other factors apart from coral heterotrophy. Some studies have found a connection between coral resource use and their morphology and polyp size (e.g., Porter 1976; Conti-Jerpe et al. 2020), but this is unlikely to have affected the isotopic composition of these Hawaiian corals, as no clear patterns were observed. For example, the branching corals *P. acuta* and *P. compressa* had $\delta^{15}N_{h-e}$ values that were more than 2‰ apart while *P. acuta* had nearly the same average $\delta^{15}N_{h-e}$ values as the encrusting coral *M. patula* (Table S3). Work by Palardy et al. (2005) also demonstrated that polyp size alone was not a determining factor in coral feeding rates. While the depth of coral collection was within a few meters for all corals, it is possible that different light environments (e.g., Muscatine et al. 1989; Ziegler et al. 2014; Wall et al. 2020) within and among the collection sites could influence the isotopic composition of these corals. Finally, natural variability in biomass, lipid levels, and lipid classes (Rodrigues et al. 2008; R. McLachlan unpubl.) may influence the isotopic composition of a coral (Rodrigues et al. 2008; Wall et al. 2019) and should be considered when using $\delta^{13}C_{h-e}$ and $\delta^{15}N_{h-e}$ as tools for estimating the proportionate contribution of heterotrophy and photoautotrophy.

Approach 3: Stable isotope Bayesian ellipses

The overlap between the host and algal endosymbiont overall isotopic composition calculated via SIBER suggests that corals utilize a variety of trophic strategies (Figs. 2, 6C). High degrees of overlap for the 40% SEA_C in *M. capitata*, *P. meandrina*, and *P. lobata* indicate a relatively low proportionate contribution of heterotrophy and high degree of resource sharing between the host and algal endosymbionts. Conversely, the 0–1% overlap in the 40% SEA_C of *M. patula* and *P. evermanni* suggests a high proportionate contribution of heterotrophy and a greater disconnect between the host tissue and algal endosymbiont. Unlike the findings by Conti-Jerpe et al. (2020) where differences between the host and algal endosymbionts were more often restricted to $\delta^{15}N$, here variability was observed in both the $\delta^{13}C$ and $\delta^{15}N$ isotope space (Fig. 2). For example, the $\delta^{15}N$ of the host tissue in the *Porites* corals was often depleted relative to the algal endosymbiont but both fractions had similar $\delta^{13}C$ values (Supporting

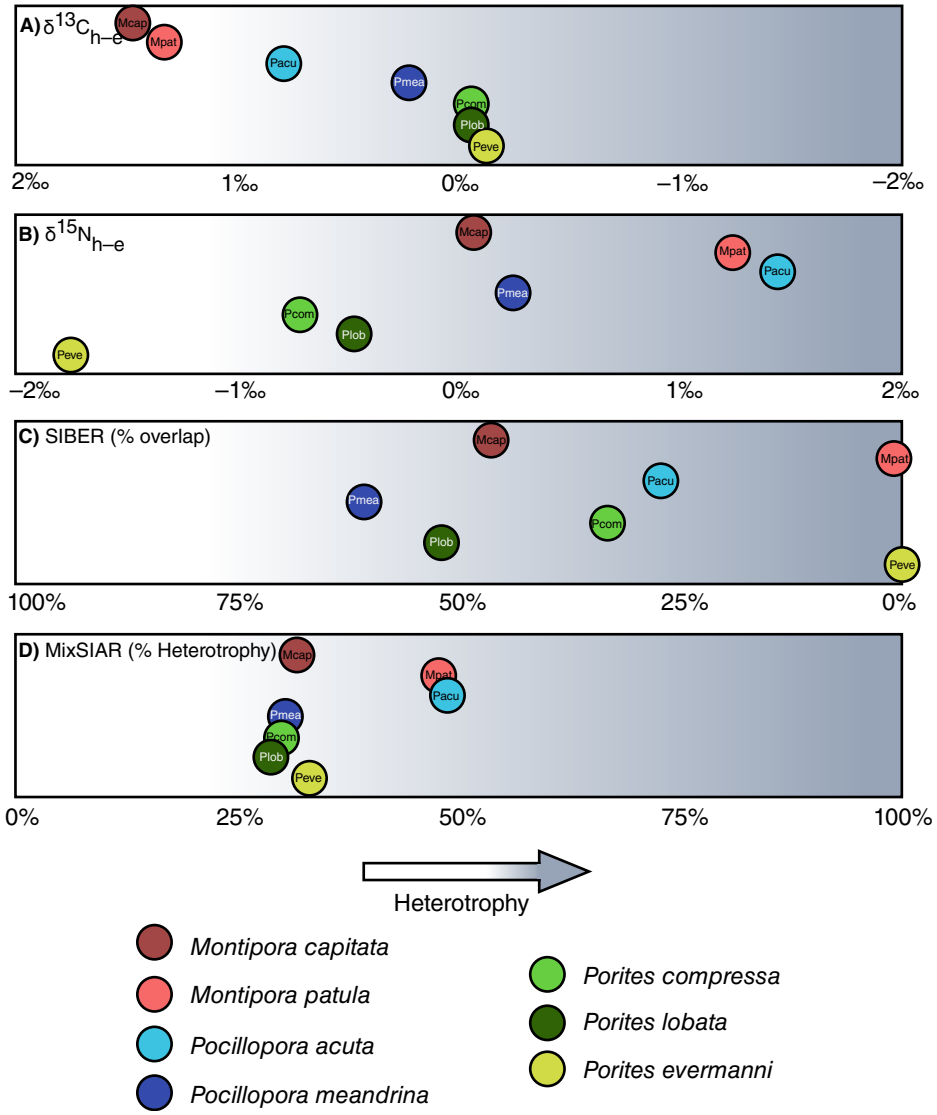

Fig. 6. A gradient showing patterns in the four approaches used to estimate the proportionate contribution of heterotrophy to Hawaiian coral tissue. The mean value for each coral species using each approach, (**A**) $\delta^{13}C_{h-e}$ (Supporting Information Table S3), (**B**) $\delta^{15}N_{h-e}$ (Supporting Information Table S4), (**C**) SIBER (overlap of 40% SEA_C, Fig. 2), and (**D**) MixSIAR (Supporting Information Table S8), is presented on the x-axis and values are ordered on the y-axis by species. The relative heterotrophic contribution increases from left to right following the arrow, based on the most common interpretation of each approach in previous studies.

Information Tables S3, S4), which resulted in negative $\delta^{15}N_{h-e}$ values and $\delta^{13}C_{h-e}$ near 0‰ (Fig. 6A,B). In the most extreme case with *P. evermanni*, this produced a 0.0% overlap of the 40% host and algal endosymbiont SEA_C (Figs. 2G, 6C). In contrast, *M. patula* coral had high $\delta^{13}C_{h-e}$ and $\delta^{15}N_{h-e}$ values (Fig. 6A,B) that also resulted in a minimal 1.1% overlap of the 40% host and algal endosymbiont SEA_C (Figs. 2B, 6C) but in a completely different way than for *P. evermanni*. The consistently low host $\delta^{15}N$ values compared to the algal endosymbionts in *P. evermanni*, and to a lesser extent in the other two poritid species, may indicate a greater incorporation of $\delta^{15}N$ depleted mucus-associated bacteria (Montoya et al. 2002). The contribution of diazotrophs to coral tissue is variable among species and locations (e.g., Lesser et al. 2007; Alamaru et al. 2009; Radice et al. 2019) but could be a source of depleted $\delta^{15}N$ for the host tissue in the *Porites* corals. The opposite pattern was observed in the $\delta^{13}C$ and $\delta^{15}N$ values of *M. patula* (Figs. 2B, 6A,B), but the enriched $\delta^{15}N$ of the host tissues relative to the endosymbiont suggests that the contribution of organic matter and zooplankton to tissues in this coral is relatively high.

However, the minimal overlap in the ellipses for *M. patula* and *P. evermanni* is not meant to suggest a complete absence of resource sharing between the host and algal endosymbiont.

The mixotrophic nature of these Hawaiian corals is well established. Indeed, when considering the 95% SEA_C overlap (Fig. 2), it is apparent that there is not a complete disconnect between the host and algal endosymbiont in these species. Rather, for these Hawaiian corals, SIBER can be a tool used to estimate the relative amount of resources shared and incorporated between the coral host and algal endosymbiont, similar to $\delta^{13}C_{h-e}$ and $\delta^{15}N_{h-e}$.

Approach 4: Bayesian mixing models

Bayesian mixing models via MixSIAR were used to specifically estimate the contribution of DIM and heterotrophic sources (POM and zooplankton) to whole coral tissue (host and algal endosymbiont). With the incorporation of uncertainty in both source values and trophic enrichment factors, mixing models present a conservative estimate of trophic strategies among Hawaiian corals. Further, DOM was excluded as a source from these models due to less reliable measurements and likely comprises a portion of the estimated contribution attributed to POM. Overall, when considering models with the typical consumer trophic enrichment of 1‰ for $\delta^{13}C$ and 3.4‰ for $\delta^{15}N$, coral species were estimated to derive a mean of 28.7–49.3% (median of 32.7%) of their tissues from heterotrophic sources (Figs. 5, 6D; Supporting Information Table S8), with additional variability among sites. This is consistent with previous findings that healthy corals typically meet 5–50% of metabolic demand heterotrophically (e.g., Grottoli et al. 2006; Tremblay et al. 2011; Grottoli et al. 2014) and that some species and/or populations can utilize greater amounts of heterotrophically derived C for tissue and lipid synthesis, especially following bleaching (Hughes et al. 2010; Hughes and Grottoli 2013; Baumann et al. 2014).

The two coral species estimated to rely most on heterotrophy, primarily via incorporation of POM, were *P. acuta* and *M. patula* at approximately 50% (Figs. 4B,C, 5B,C, 6D). Although heterotrophy in these two coral species has not previously been studied in Hawai‘i, research on corals of the *Pocillopora* and *Montipora* genera show that both can effectively feed on zooplankton and capture POM, though the proportions vary among locations, local environmental conditions, and health status (Anthony 1999; Palardy et al. 2005, 2008). Interestingly, *P. acuta* and *M. patula* were estimated to incorporate approximately 15% more heterotrophically derived sources into their tissues than their congeners, *P. meandrina* and *M. capitata*. Both *P. meandrina* and *M. capitata* are flexible in their incorporation of heterotrophically derived organic matter depending on environmental conditions (Fox et al. 2018) and health status (Grottoli et al. 2006; Palardy et al. 2008), respectively. It is unclear what might drive these intrageneric differences in heterotrophy, but increased heterotrophic capacity through POM or DOM uptake may contribute to the rapid recruitment and growth of *P. acuta* colonies in warmer ocean conditions (Bahr et al. 2020), or aid encrusting *M. patula* corals to compete for space in turbid environments (Brown and Friedlander 2007).

P. lobata had the lowest mean proportionate contribution of heterotrophically derived organic matter in its tissues at 28.7% (Table S8G), although *P. compressa* (29.7%) and *M. capitata* (31.6%) had similarly low estimates of heterotrophic contribution. This appears contradictory to past evidence showing that this species has an elevated baseline feeding capacity relative to *P. compressa* and *M. capitata* (Palardy et al. 2008) and the capacity to take up dissolved organic carbon as a nutritional source (Levas et al. 2013). However, past studies of this species did not include POM as a source. Further, the sources allocated for tissue building and energy storage, which drives the tissue isotopic composition, may be different from what is used for fulfilling daily energetic demands (e.g., Wall et al. 2019). For example, nonbleached *P. compressa* incorporates similar levels of heterotrophically derived C into its tissues as *M. capitata* (Hughes et al. 2010; Baumann et al. 2014) even though its feeding capacity is higher than that of *M. capitata* (Palardy et al. 2008). The low heterotrophic contribution to tissues in *P. lobata* suggests that heterotrophically acquired organic matter contributes more to meeting metabolic demand than to tissue building. This is plausible, given that healthy Hawaiian *P. lobata* can meet 45% of metabolic demand from heterotrophy alone and that Caribbean *P. astreoides* can meet up to 70% this way (Palardy et al. 2008; Levas et al. 2016). Heterotrophically acquired nutrition has also been observed to support 100% of metabolic demand in bleached *M. capitata* and bleached *P. astreoides*, providing a vital strategy for resilience postbleaching (Grottoli et al. 2006; Hughes et al. 2010; Levas et al. 2016). While lower than expected, our findings provide further evidence that *P. lobata* utilizes heterotrophically acquired organic matter for meeting metabolic demand, possibly accounting for its resilience to bleaching compared to many other coral species (e.g., Hueerkamp et al. 2001; Kenyon et al. 2006).

Due to intense recycling of organic matter between the coral host and its algal endosymbiont, it is possible that there is minimal fractionation offset in $\delta^{13}C$ and $\delta^{15}N$ between the two symbiotic partners. When TDF in both $\delta^{13}C$ and $\delta^{15}N$ for all heterotrophic sources was reduced to 0.0‰, the mean proportionate contribution of zooplankton across coral species increased substantially from 3.0% to 21.3% (Supporting Information Tables S8B–H, S9B–H), suggesting that zooplankton may be more valuable to coral tissues than estimated by the primary mixing models in this study. Nevertheless, with either model scenario DIM still comprises two-thirds of the estimated contribution to coral tissues on average (Supporting Information Tables S8, S9).

Finally, the contribution of heterotrophic sources to coral tissues varied among sites for some coral species (Supporting Information Table S8B–H; Fig. 4). For example, nearly 50% of *M. capitata* tissues are derived from heterotrophic sources at HIMB, but only 9.6% are heterotrophically derived in Hale‘iwa

(Supporting Information Table S8). However, the contribution of heterotrophic sources to *P. acuta* tissues was estimated to be approximately 45–55% at both HIMB and Haleʻiwa (Supporting Information Table S8D). The $\delta^{15}N$ values were also greatly enriched at in *P. acuta* from Waimānalo (Fig. 4), but it is unclear what drives this underlying enrichment as a similar pattern was not observed in any other coral species. Thus, the proportionate contribution of heterotrophic sources to coral tissues was not dependent on site, but on the interaction between coral species and site-specific environmental effects.

There are potential caveats to this Bayesian mixing model approach that must be considered. Due to logistical constraints, the source sampling occurred in December 2017, approximately 2 yr following the collection of the corals, which could mean the source values do not completely match what was available to the corals prior to their collection. In addition, $\delta^{15}N$ of DIN was estimated based on published values in Kāneʻohe Bay (Wall et al. 2019), which may not represent the actual DIN values at each site. Kāneʻohe Bay is a semi-enclosed body of water and the corals in this bay can be exposed to greater amounts of terrestrial runoff than at other sites, potentially affecting their isotopic composition. Indeed, even the genetic structure of Hawaiian *Porites* corals is known to differ along gradients of anthropogenic influence (Tisthammer et al. 2020). Changes in the concentration of DIM are also important considerations, as natural seasonal fluctuations and variation in anthropogenic influence can affect the fractionation of $\delta^{13}C$ and $\delta^{15}N$ used for photosynthesis (Swart et al. 2005, further explanation of fractionation values used in the mixing models is included in the Supporting Information). Therefore, while these mixing models incorporate a range of values to provide a reasonable estimate of sources around the island of Oʻahu as a whole, it is possible that the models do not always encompass the full range of isotopic composition for inorganic nutrients like DIN.

Comparing approaches

While each of the four approaches (i.e., $\delta^{13}C_{h-e}$, $\delta^{15}N_{h-e}$, SIBER, and MixSIAR) provided a useful measure of photoautotrophic and heterotrophic contributions to coral tissues in past studies, our direct comparison of these approaches reveals previously unrecognized differences in their interpretations (Fig. 6). Though not statistically significant, both the mean $\delta^{13}C_{h-e}$ and $\delta^{15}N_{h-e}$ for each species tended to increase as the proportionate contribution from heterotrophic sources derived from MixSIAR increased (Supporting Information Fig. S2A,B), while the isotopic niche overlap calculated via SIBER displayed the opposite relationship (Supporting Information Fig. S2C). The positive relationship between proportionate contribution estimated via mixing models and $\delta^{13}C_{h-e}$ contradicts past evidence that $\delta^{13}C_{h-e}$ typically decreases with greater heterotrophic contributions (e.g., Rodrigues and Grottoli 2006; Fox et al. 2018), suggesting that $\delta^{13}C_{h-e}$ in natural Hawaiian corals may not be comparable among species. Here, $\delta^{13}C_{h-e}$ appears useful for comparisons within species, such as heterotrophic contribution among sites (Fig. 1), across depth gradients (e.g., Muscatine et al. 1989; Alamaru et al. 2009; Williams et al. 2018), or following bleaching events (e.g., Rodrigues and Grottoli 2006; Wall et al. 2019). The strongest correlation was between the mixing model output and $\delta^{15}N_{h-e}$ (Supporting Information Fig. S2), matching previously described relationships with heterotrophy (e.g., Conti-Jerpe et al. 2020). Interestingly, the relationship between the mixing model output and the niche overlap calculated via SIBER was weaker than with $\delta^{15}N_{h-e,}$ which may be an artifact of the unexpected $\delta^{15}N$ enrichment of the algal endosymbionts relative to the host in the poritid corals, particularly *P. evermanni*. Together, this suggests that if measurements for sources like DIM, POM, and zooplankton were not available, all three approaches could provide some measure of the relative contribution of heterotrophy to corals, but $\delta^{15}N_{h-e}$ appears to be more closely related to heterotrophy in Hawaiian corals based on the mixing models used here.

The mixing models also require some caution in their interpretation, because changes in the fractionation assumptions and the possible contribution of unmeasured sources (e.g., diazotrophically fixed nitrogen) could lead to different conclusions. Irrespective of the approach used, for known resilient species like *P. lobata*, the low heterotrophic contribution to coral tissues does not always align with known higher feeding capacity, indicating that heterotrophic contribution to coral tissues is only one of many tools for evaluating the underlying drivers of coral resilience to changing ocean conditions associated with global climate change. However, the inconsistencies among approaches here using bulk $\delta^{13}C$ and $\delta^{15}N$ suggest that more work is needed and future investigations should consider using promising techniques like compound-specific isotope analyses targeting essential amino acids, as these methods could more precisely identify the diversity of trophic strategies used by corals.

References

Alamaru, A., Y. Loya, E. Brokovich, R. Yam, and A. Shemesh. 2009. Carbon and nitrogen utilization in two species of Red Sea corals along a depth gradient: Insights from stable isotope analysis of total organic material and lipids. Geochim. Cosmochim. Acta **73**: 5333–5342. doi:10.1016/j.gca.2009.06.018

Anthony, K. R. N. 1999. Coral suspension feeding on fine particulate matter. J. Exp. Mar. Biol. Ecol. **232**: 85–106. doi:10.1016/S0022-0981(98)00099-9

Anthony, K. R. N., and K. E. Fabricius. 2000. Shifting roles of heterotrophy and autotrophy in coral energetics under varying turbidity. J. Exp. Mar. Biol. Ecol. **252**: 221–253. doi:10.1016/S0022-0981(00)00237-9

Anthony, K. R. N., M. O. Hoogenboom, J. A. Maynard, A. G. Grottoli, and R. Middlebrook. 2009. Energetics approach to predicting mortality risk from environmental stress: A case study of coral bleaching. Funct. Ecol. **23**: 539–550. doi:10.1111/j.1365-2435.2008.01531.x

Bahr, K. D., T. Tran, C. P. Jury, and R. J. Toonen. 2020. Abundance, size, and survival of recruits of the reef coral *Pocillopora acuta* under ocean warming and acidification. PLoS One **15**: e0228168. doi:10.1371/journal.pone.0228168

Baumann, J., A. G. Grottoli, A. D. Hughes, and Y. Matsui. 2014. Photoautotrophic and heterotrophic carbon in bleached and non-bleached coral lipid acquisition and storage. J. Exp. Mar. Biol. Ecol. **461**: 469–478. doi:10.1016/j.jembe.2014.09.017

Baums, I. B., and others. 2019. Considerations for maximizing the adaptive potential of restored coral populations in the western Atlantic. Ecol. Appl. **29**: e01978. doi:10.1002/eap.1978

Brown, E., and A. Friedlander. 2007. Spatio-temporal patterns in coral cover and coral settlement on an exposed shoreline in Hawai'i, p. 10–12. *In* M. E. Field, C. J. Berg and S. A. Cochran (eds.), Science and management in the Hanalei Watershed: A trans-disciplinary approach. USGS Open File Report.

Conti-Jerpe, I. E., P. D. Thompson, C. W. M. Wong, N. L. Oliveira, N. N. Duprey, M. A. Moynihan, and D. M. Baker. 2020. Trophic strategy and bleaching resistance in reef-building corals. Sci. Adv. **6**: eaaz5443. doi:10.1126/sciadv.aaz5443

Edmunds, P. J., and P. S. Davies. 1989. An energy budget for *Porites porites* (Scleractinia), growing in a stressed environment. Coral Reefs **8**: 37–43. doi:10.1007/BF00304690

Ferrier-Pagès, and others. 2011. Summer autotrophy and winter heterotrophy in the temperate symbiotic coral *Cladocora caespitosa*. Limnol. Oceanogr. **56**: 1429–1438. doi:10.4319/lo.2011.56.4.1429

Ferrier-Pagès, C., S. Martinez, R. Grover, J. Cybulski, E. Shemesh, and D. Tchernov. 2021. Tracing the trophic plasticity of the coral-dinoflagellate symbiosis using amino acid compound-specific stable isotope analysis. Microorganisms **9**: 182. doi:10.3390/microorganisms9010182

Fox, M. D., and others. 2018. Gradients in primary production predict trophic strategies of mixotrophic corals across spatial scales. Curr. Biol. **28**: 3355–3363. doi:10.1016/j.cub.2018.08.057

Fox, M. D., E. A. Elliot Smith, J. E. Smith, and S. D. Newsome. 2019. Trophic plasticity in a common reef-building coral: Insights from $\delta^{13}C$ analysis of essential amino acids. Funct. Ecol. **33**: 2203–2214. doi:10.1111/1365-2435.13441

Fujii, T., Y. Tanaka, K. Maki, N. Saotome, N. Morimoto, A. Watanabe, and T. Miyajima. 2020. Organic carbon and nitrogen isoscapes of reef corals and algal symbionts: Relative influences of environmental gradients and heterotrophy. Microorganisms **8**: 1221. doi:10.3390/microorganisms8081221

Grottoli, A. G. 2020. Carbon and nitrogen stable isotopes of Hawaiian corals collected from August to November 2015. Biological and Chemical Oceanography Data Management Office (BCO-DMO). (Version 1) Version Date 2020-10-26. doi:10.26008/1912/bco-dmo.827587.1

Grottoli, A. G. 2021. Carbon and nitrogen stable isotopes of marine inorganic and organic matter around O'ahu, Hawai'i, December 2017. Biological and Chemical Oceanography Data Management Office (BCO-DMO). (Version 1) Version Date 2021-03-11. doi:10.26008/1912/bco-dmo.844810.1

Grottoli, A. G., L. J. Rodrigues, and J. E. Palardy. 2006. Heterotrophic plasticity and resilience in bleached corals. Nature **440**: 1186–1189. doi:10.1038/nature04565

Grottoli, A. G., M. E. Warner, S. J. Levas, M. D. Aschaffenburg, V. Schoepf, M. McGinley, J. Baumann, and Y. Matsui. 2014. The cumulative impact of annual coral bleaching can turn some coral species winners into losers. Glob. Chang. Biol. **20**: 3823–3833. doi:10.1111/gcb.12658

Grottoli, A. G., D. Tchernov, and G. Winters. 2017. Physiological and biogeochemical responses of super-corals to thermal stress from the Northern Gulf of Aqaba, Red Sea. Front. Mar. Sci. **4**: 215. doi:10.3389/fmars.2017.00215

Houlbrèque, F., and C. Ferrier-Pagès. 2009. Heterotrophy in tropical scleractinian corals. Biol. Rev. **84**: 1–17. doi:10.1111/j.1469-185X.2008.00058.x

Hueerkamp, C., P. W. Glynn, L. D'Croz, J. L. Maté, and S. B. Colley. 2001. Bleaching and recovery of five eastern Pacific corals in an El Niño-related temperature experiment. Bull. Mar. Sci. **69**: 215–236.

Hughes, A. D., A. G. Grottoli, T. Pease, and Y. Matsui. 2010. Acquisition and assimilation of carbon in non-bleached and bleached corals. Mar. Ecol. Prog. Ser. **420**: 91–101. doi:10.3354/meps08866

Hughes, A. D., and A. G. Grottoli. 2013. Heterotrophic compensation: A possible mechanism for resilience of coral reefs to global warming or a sign of prolonged stress? PLoS One **8**: 81172. doi:10.1371/journal.pone.0081172

Jackson, A. L., R. Inger, A. C. Parnell, and S. Bearhop. 2011. Comparing isotopic niche widths among and within communities: SIBER - Stable Isotope Bayesian Ellipses in R. J. Anim. Ecol. **80**: 595–602. doi:10.1111/j.1365-2656.2011.01806.x

Kenyon, J., G. S. Aeby, R. E. Brainard, J. D. Chojnacki, M. J. Dunlap, and C. B. Wilkinson. 2006. Mass coral bleaching on high-latitude reefs in the Hawaiian Archipelago, p. 631–643. In *Proceedings of the 10th International Coral Reef Symposium*, Okinawa, Japan.

Krueger, T., J. Bodin, N. Horwitz, C. Loussert-Fonta, A. Sakr, S. Escrig, M. Fine, and A. Meibom. 2018. Temperature and feeding induce tissue level changes in autotrophic and heterotrophic nutrient allocation in the coral symbiosis – a

NanoSIMS study. Sci. Rep. **8**: 1–15. doi:10.1038/s41598-018-31094-1

LaJeunesse, T. C., D. J. Thornhill, E. F. Cox, F. G. Stanton, W. K. Fitt, and G. W. Schmidt. 2004. High diversity and host specificity observed among symbiotic dinoflagellates in reef coral communities from Hawaii. Coral Reefs **23**: 596–603. doi:10.1007/s00338-004-0428-4

LaJeunesse, T. C., J. E. Parkinson, P. W. Gabrielson, H. J. Jeong, J. D. Reimer, C. R. Voolstra, and S. R. Santos. 2018. Systematic revision of Symbiodiniaceae highlights the antiquity and diversity of coral endosymbionts. Curr. Biol. **28**: 2570–2580. doi:10.1016/j.cub.2018.07.008

Lesser, M., L. Falcón, A. Rodríguez-Román, S. Enríquez, O. Hoegh-Guldberg, and R. Iglesias-Prieto. 2007. Nitrogen fixation by symbiotic cyanobacteria provides a source of nitrogen for the scleractinian coral *Montastraea cavernosa*. Mar. Ecol. Prog. Ser. **346**: 143–152. doi:10.3354/meps07008

Levas, S., A. G. Grottoli, V. Schoepf, M. Aschaffenburg, J. Baumann, J. E. Bauer, and M. E. Warner. 2016. Can heterotrophic uptake of dissolved organic carbon and zooplankton mitigate carbon budget deficits in annually bleached corals? Coral Reefs **35**: 495–506. doi:10.1007/s00338-015-1390-z

Levas, S., V. Schoepf, M. E. Warner, M. Aschaffenburg, J. Baumann, and A. G. Grottoli. 2018. Long-term recovery of Caribbean corals from bleaching. J. Exp. Mar. Biol. Ecol. **506**: 124–134. doi:10.1016/j.jembe.2018.06.003

Levas, S. J., A. G. Grottoli, A. D. Hughes, C. L. Osburn, and Y. Matsui. 2013. Physiological and biogeochemical traits of bleaching and recovery in the mounding species of coral *Porites lobata*: Implications for resilience in mounding corals. PLoS One **8**: 63267. doi:10.1371/journal.pone.0063267

Minagawa, M., and E. Wada. 1984. Stepwise enrichment of ^{15}N along food chains: Further evidence and the relation between δ^{15}N and animal age. Geochim. Cosmochim. Acta **48**: 1135–1140. doi:10.1016/0016-7037(84)90204-7

Montoya, J. P., E. J. Carpenter, and D. G. Capone. 2002. Nitrogen fixation and nitrogen isotope abundances in zooplankton of the oligotrophic North Atlantic. Limnol. Oceanogr. **47**: 1617–1628. doi:10.4319/lo.2002.47.6.1617

Moyer, R. P., J. E. Bauer, and A. G. Grottoli. 2013. Carbon isotope biogeochemistry of tropical small mountainous river, estuarine, and coastal systems of Puerto Rico. Biogeochemistry **112**: 589–612. doi:10.1007/s10533-012-9751-y

Muscatine, L., and J. W. Porter. 1977. Reef corals: Mutualistic symbioses adapted to nutrient-poor environments. Bioscience **27**: 454–460. doi:10.2307/1297526

Muscatine, L., P. G. Falkowski, J. W. Porter, and Z. Dubinsky. 1984. Fate of photosynthetic fixed carbon in light- and shade-adapted colonies of the symbiotic coral *Stylophora pistillata*. Proc. R. Soc. B **222**: 181–202. doi:10.1098/rspb.1984.0058

Muscatine, L., J. W. Porter, and I. R. Kaplan. 1989. Resource partitioning by reef corals as from stable isotope composition I. δ^{13}C of zooxanthellae and animal tissue vs depth determined. Mar. Biol. **100**: 185–193. doi:10.1007BF00391957

Muscatine, L., and I. R. Kaplan. 1994. Resource partitioning by reef corals as determined from stable isotope composition II. δ^{15}N of zooxanthellae and animal tissue versus depth. Pac. Sci. **48**: 304–312.

Nahon, S., N. B. Richoux, J. Kolasinski, M. Desmalades, C. Ferrier-Pagès, G. Lecellier, S. Planes, and V. Berteaux Lecellier. 2013. Spatial and temporal variations in stable carbon (δ^{13}C) and nitrogen (δ^{15}N) isotopic composition of symbiotic scleractinian corals. PLoS One **8**: e81247. doi:10.1371/journal.pone.0081247

Palardy, J. E., A. G. Grottoli, and K. A. Matthews. 2005. Effects of upwelling, depth, morphology and polyp size on feeding in three species of Panamanian corals. Mar. Ecol. Prog. Ser. **300**: 79–89. doi:10.3354/meps300079

Palardy, J. E., A. G. Grottoli, and K. A. Matthews. 2006. Effect of naturally changing zooplankton concentrations on feeding rates of two coral species in the Eastern Pacific. J. Exp. Mar. Biol. Ecol. **331**: 99–107. doi:10.1016/j.jembe.2005.10.001

Palardy, J. E., L. J. Rodrigues, and A. G. Grottoli. 2008. The importance of zooplankton to the daily metabolic carbon requirements of healthy and bleached corals at two depths. J. Exp. Mar. Biol. Ecol. **367**: 180–188. doi:10.1016/j.jembe.2008.09.015

Piniak, G., F. Lipschultz, and J. McClelland. 2003. Assimilation and partitioning of prey nitrogen within two anthozoans and their endosymbiotic zooxanthellae. Mar. Ecol. Prog. Ser. **262**: 125–136. doi:10.3354/meps262125

Porter, J. W. 1976. Autotrophy, heterotrophy, and resource partitioning in Caribbean reef-building corals. Am. Nat. **110**: 731–742. doi:10.1086/283100

Post, D. M. 2002. Using stable isotopes to estimate trophic position: Models, methods, and assumptions. Ecology **83**: 703–718. doi:10.2307/3071875

Price, J. T., A. Smith, K. L. Dobson, and A. G. Grottoli. 2020. Airbrushed coral sample preparation for organic stable carbon and nitrogen isotope analyses. protocols.io. doi:10.17504/protocols.io.bgi7juhn

R Core Team. 2020. R: A language and environment for statistical computing. R Foundation for Statistical Computing, Vienna, Austria. https://www.R-project.org/

Radice, V. Z., O. Hoegh-Guldberg, B. Fry, M. D. Fox, and S. G. Dove. 2019. Upwelling as the major source of nitrogen for shallow and deep reef-building corals across an oceanic atoll system. Funct. Ecol. **33**: 1120–1134. doi:10.1111/1365-2435.13314

Rangel, M. S., D. Erler, A. Tagliafico, K. Cowden, S. Scheffers, and L. Christidis. 2019. Quantifying the transfer of prey δ^{15}N signatures into coral holobiont nitrogen pools. Mar. Ecol. Prog. Ser. **610**: 33–49. doi:10.3354/meps12847

Reynaud, S., P. Martinez, F. Houlbrèque, I. Billy, D. Allemand, and C. Ferrier-Pagès. 2009. Effect of light and feeding on the nitrogen isotopic composition of a zooxanthellate coral: Role of nitrogen recycling. Mar. Ecol. Prog. Ser. **392**: 103–110. doi:10.3354/meps08195

Ribes, M., and M. J. Atkinson. 2007. Effects of water velocity on picoplankton uptake by coral reef communities. Coral Reefs **26**: 413–421. doi:10.1007/s00338-007-0211-4

Rodrigues, L. J., and A. G. Grottoli. 2006. Calcification rate and the stable carbon, oxygen, and nitrogen isotopes in the skeleton, host tissue, and zooxanthellae of bleached and recovering Hawaiian corals. Geochim. Cosmochim. Acta **70**: 2781–2789. doi:10.1016/j.gca.2006.02.014

Rodrigues, L. J., A. G. Grottoli, and T. K. Pease. 2008. Lipid class composition of bleached and recovering *Porites compressa* Dana, 1846 and *Montipora capitata* Dana, 1846 corals. Hawai'i. J. Exp. Mar. Biol. Ecol. **358**: 136–143. doi:10.1016/j.jembe.2008.02.004

Santos, M. E. A., D. M. Baker, I. E. Conti-Jerpe, and J. D. Reimer. 2021. Populations of a widespread hexacoral have trophic plasticity and flexible synthrophic interactions across the Indo-Pacific Ocean. Coral Reefs. doi:10.1007/s00338-021-02055-4

Schoepf, V., A. G. Grottoli, S. J. Levas, M. D. Aschaffenburg, J. H. Baumann, Y. Matsui, and M. E. Warner. 2015. Annual coral bleaching and the long-term recovery capacity of coral. Proc. R. Soc. B **282**: 20151887. doi:10.1098/rspb.2015.1887

Stock, B. C., A. L. Jackson, E. J. Ward, A. C. Parnell, D. L. Phillips, and B. X. Semmens. 2018. Analyzing mixing systems using a new generation of Bayesian tracer mixing models. PeerJ **2018**: e5096. doi:10.7717/peerj.5096

Swart, P. K., A. Szmant, J. W. Porter, R. E. Dodge, J. I. Tougas, and J. R. Southam. 2005. The isotopic composition of respired carbon dioxide in scleractinian corals: Implications for cycling of organic carbon in corals. Geochim. Cosmochim. Acta **69**: 1495–1509. doi:10.1016/j.gca.2004.09.004

Tanaka, Y., A. G. Grottoli, Y. Matsui, A. Suzuki, and K. Sakai. 2015. Partitioning of nitrogen sources to algal endosymbionts of corals with long-term ^{15}N-labelling and a mixing model. Ecol. Model. **309–310**: 163–169. doi:10.1016/j.ecolmodel.2015.04.017

Tanaka, Y., A. Suzuki, and K. Sakai. 2018. The stoichiometry of coral-dinoflagellate symbiosis: Carbon and nitrogen cycles are balanced in the recycling and double translocation system. ISME J. **12**: 860–868. doi:10.1038/s41396-017-0019-3

Tisthammer, K. H., Z. H. Forsman, R. J. Toonen, and R. H. Richmond. 2020. Genetic structure is stronger across human-impacted habitats than among islands in the coral *Porites lobata*. PeerJ **8**: e8550. doi:10.7717/peerj.8550

Tremblay, P., A. Peirano, and C. Ferrier-Pagès. 2011. Heterotrophy in the Mediterranean symbiotic coral *Cladocora caespitosa*: Comparison with two other scleractinian species. Mar. Ecol. Prog. Ser. **422**: 165–177. doi:10.3354/meps08902

Tremblay, P., R. Grover, J. F. Maguer, L. Legendre, and C. Ferrier-Pagès. 2012. Autotrophic carbon budget in coral tissue: A new ^{13}C-based model of photosynthate translocation. J. Exp. Biol. **215**: 1384–1393. doi:10.1242/jeb.065201

Wall, C. B., R. Ritson-Williams, B. N. Popp, and R. D. Gates. 2019. Spatial variation in the biochemical and isotopic composition of corals during bleaching and recovery. Limnol. Oceanogr. **64**: 2011–2028. doi:10.1002/lno.11166

Wall, C. B., M. Kaluhiokalani, B. N. Popp, M. J. Donahue, and R. D. Gates. 2020. Divergent symbiont communities determine the physiology and nutrition of a reef coral across a light-availability gradient. ISME J. **14**: 945–958. doi:10.1038/s41396-019-0570-1

Wijgerde, T., P. Spijkers, E. Karruppannan, J. A. J. Verreth, and R. Osinga. 2012. Water flow affects zooplankton feeding by the scleractinian coral *Galaxea fascicularis* on a polyp and colony level. J. Mar. Sci. **2012**: 854849. doi:10.1155/2012/854849

Williams, G. J., and others. 2018. Biophysical drivers of coral trophic depth zonation. Mar. Biol. **165**: 1–15. doi:10.1007/s00227-018-3314-2

Xu, S., and others. 2020. Intergeneric differences in trophic status of scleractinian corals from Weizhou Island, northern South China Sea: Implication for their different environmental stress tolerance. J. Geophys. Res. Biogeosci. **125**: e2019JG005451. doi:10.1029/2019JG005451

Ziegler, M., C. M. Roder, C. Büchel, and C. R. Voolstra. 2014. Limits to physiological plasticity of the coral *Pocillopora verrucosa* from the central Red Sea. Coral Reefs **33**: 1115–1129. doi:10.1007/s00338-014-1192-8

Acknowledgments

We thank the Hawai'i Institute of Marine Biology for logistical support. We also thank J. Altuscher, K. Dobson, H. Hayes, C. Juracka, E. Kline, L. Mullins, and A. Smith for their laboratory assistance. We also thank E. Geiger and S. Heron for their assistance with obtaining the satellite environmental data. Major funding for this work was provided to AGG by the National Science Foundation (Award 1459536 and 1838667) and the Herbert W. Hoover Foundation and to RJT by the National Science Foundation (1416889). Additional funding was provided to JTP by the Geological Society of America and the Ohio State University.

Conflict of Interest

None declared.

Submitted 21 August 2020
Revised 31 January 2021
Accepted 17 March 2021

Associate editor: Steeve Comeau